Electronic Supplementary Material (ESI) for Chemical Communications
This journal is © The Royal Society of Chemistry 2012

Hysteretic CO_2 sorption in a novel copper(II)-indazole-carboxylate porous coordination polymer

Chris S Hawes*, Ravichandar Babarao, Matthew Hill, Keith White, Brendan F. Abrahams and Paul E. Kruger*

Electronic Supporting Information (ESI)

This journal is © The Royal Society of Chemistry 2012

Experimental

General Considerations

All synthetic transformations were carried out using commercially available reagents and starting materials, and were carried out in air unless otherwise specified. Anhydrous solvents were prepared by passing HPLC-grade solvent through a sealed column of activated alumina. NMR spectra were collected on a Varian INOVA spectrometer operating at 500 MHz for ^{1}H and 125 MHz for ^{13}C nuclei, and are referenced to the residual solvent peaks. Mass spectra were collected on a Bruker MaXis 4G Electrospray mass spectrometer operating in positive ion mode. Melting points were collected on an Electrothermal melting point apparatus and are uncorrected. Thermogravimetric analyses were carried out on an Alphatec Q600 SDT TGA/DSC instrument using alumina crucibles, where samples were heated at a rate of 1 °C/hr to 500 °C under a nitrogen flow of 100 mL/min. Infrared spectra were recorded on a Perkin-Elmer Spectrum One FTIR spectrometer operating in diffuse reflectance mode, with samples prepared as KBr mulls. Microanalysis was carried out at the Campbell Microanalytical Laboratory, University of Otago, New Zealand. Solvothermal reactions were carried out within Parr Instruments Teflon lined acid digestion bombs within Carbolite PF60 ovens utilising Eurotherm temperature controllers.

Synthesis of H_2L.

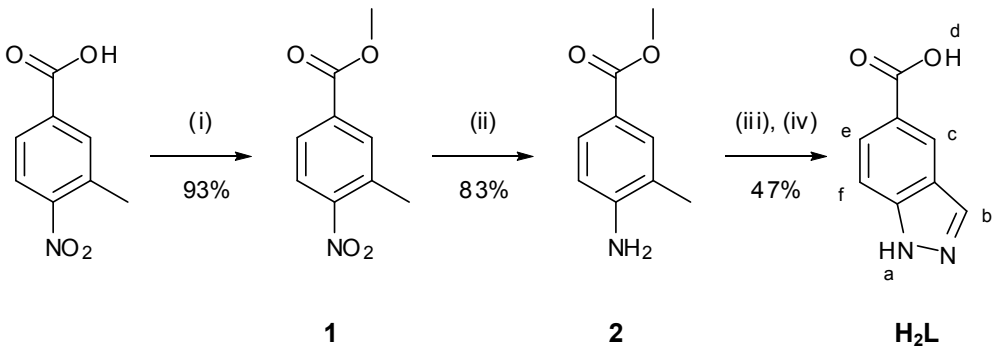

Scheme S1: Reagents and conditions: (i) MeOH, H_2SO_4 (cat.), reflux 16 hr; (ii) 10% Pd/C, NH_4HCO_2, MeOH, RT 3 hr; (iii) Ac_2O, KOAc, isoamyl nitrite, PhMe, reflux 16 hr; (iv) LiOH, THF/H_2O, reflux 48 hr, then $HCl_{(aq)}$.

Synthesis of methyl 3-methyl-4-nitrobenzoate, 1

To 3-methyl-4-nitrobenzoic acid (5 g; 28 mmol) in 30 mL methanol was added concentrated sulfuric acid (2 mL) dropwise with vigorous stirring. The resulting mixture was refluxed overnight and allowed to cool to room temperature, and then concentrated under reduced pressure. The residue was combined with 100 mL distilled water and extracted several times with dichloromethane, and the organic phases were combined, washed with water, dried with $MgSO_4$ and evaporated to dryness to give the product as a white solid. Yield 5.0 g (93%). Analytical data were found to be consistent with the commercially available material.

Synthesis of methyl 3-methyl-4-aminobenzoate, 2

The title compound was synthesised by an adaptation of the method reported by Ehrenkaufer [1]. Methyl 3-methyl-4-nitrobenzoate (2 g; 10 mmol) was dissolved in 20 mL anhydrous methanol under a nitrogen atmosphere, to which was added 10% palladium on activated carbon (500 mg) with stirring. To this mixture was added ammonium formate (3 g; 48 mmol) in one portion, and the mixture was vigorously stirred at room temperature until exothermicity and gas evolution was seen to cease (3 hours). The mixture was filtered through celite, washed with several portions of methanol, and the filtrates combined and evaporated. The residue was slurried in distilled water, and the solids were filtered and dried *in vacuo* to give the product as a white solid. Yield 1.4 g (83%). Analytical data were found to be consistent with literature values [2].

This journal is © The Royal Society of Chemistry 2012

Synthesis of 1H-indazole-5-carboxylic acid, H_2L

The title compound was prepared by an adaptation to the method reported by Hassmann [3]. To 40 mL dry toluene under a nitrogen atmosphere was added methyl 3-methyl 4-aminobenzoate (1.3 g, 7.9 mmol) and potassium acetate (400 mg, 4.1 mmol), and the mixture was heated to reflux, at which time acetic anhydride (2.3 mL, 25 mmol) was added, and the mixture was stirred at temperature for 10 minutes. Isoamyl nitrite (1.7 mL, 13 mmol) was added over 30 minutes, and the mixture was refluxed overnight. On cooling, the mixture was filtered and evaporated to dryness, to give an orange solid, which was filtered and washed with petroleum ether, giving 1.44g of methyl N-acetyl indazole-5-carboxylate. This material was taken up in 50 mL THF and added to a solution of lithium hydroxide (7 g, 290 mmol) in 50 mL water, and the resulting mixture was refluxed for 48 hours. On cooling, the mixture was concentrated on a rotary evaporator to remove THF, and the aqueous phase was filtered and taken to pH 4 with dilute hydrochloric acid, causing precipitation of the product, which was filtered, washed with water and dried *in vacuo*. Yield 600 mg (47%). MP 297–301 °C (decomp.); δ_H(500 MHz, d_6-DMSO): 7.60 (d, 1H, J = 8.8 Hz, H^f), 7.91 (dd, 1H, J^1= 8.8 Hz, J^2= 1.6 Hz, H^e), 8.24 (d, 1H, J = 0.8 Hz, H^b), 8.45 (dd, 1H, J^1 = 1.3 Hz, J^2 = 0.8 Hz, H^c), 13.2 (br s, 2H, H^d + H^a); δ_c(125 MHz, d_6-DMSO): 110.2, 122.7, 123.2, 123.9, 126.7, 135.3, 141.8, 167.8; *m/z* (ESMS): 163.0504 [M+H^+], calculated for $C_8H_7N_2O_2$ 163.0502; υ_{max}(KBr)/cm^{-1} 3297 s br, 2504 m br, 1686 s, 1622 m, 1469 w, 1357 m, 1319 s, 1269 s, 1203 m, 1134 m, 1080 m, 948 s, 768 s.

Synthesis of poly-catena-[Cu(HL)$_2$], 1

H_2L (10 mg; 61 µmol) was combined with $Cu(NO_3)_2 \cdot 3H_2O$ (4 mg; 16 µmol) and $(NH_4)_2SiF_6$ (5 mg; 28 µmol) in a 1:1 MeOH/H_2O mixture (2 mL), and added to a 23 mL Parr Instruments acid digestion bomb, which was heated to 100 °C, allowed to dwell for 24 hours, and cooled to room temperature at 4 °C/hr. The purple crystals obtained were filtered and washed sequentially with methanol, water, and a further portion of methanol, and were air dried. Yield 3.6 mg (59%); MP >300 °C; Found C, 48.6; H, 2.86; N, 13.5; $C_{48}H_{30}N_{12}O_{12}Cu_3 \cdot 2MeOH \cdot H_2O$ requires C, 48.4; H, 3.30; N, 13.6 %; υ_{max}(KBr)/cm^{-1} 3250 m; 1817 w, 1633 m, 1599 s, 1570 s, 1513 m, 1458 m, 1380 s, 1273 m, 1133 m, 1083 s, 971 s, 857 s, 793 s, 781 s, 597 m.

Figure S1: ^{1}H NMR spectrum of $\mathbf{H_2L}$ (d_6-DMSO @ 500 MHz):

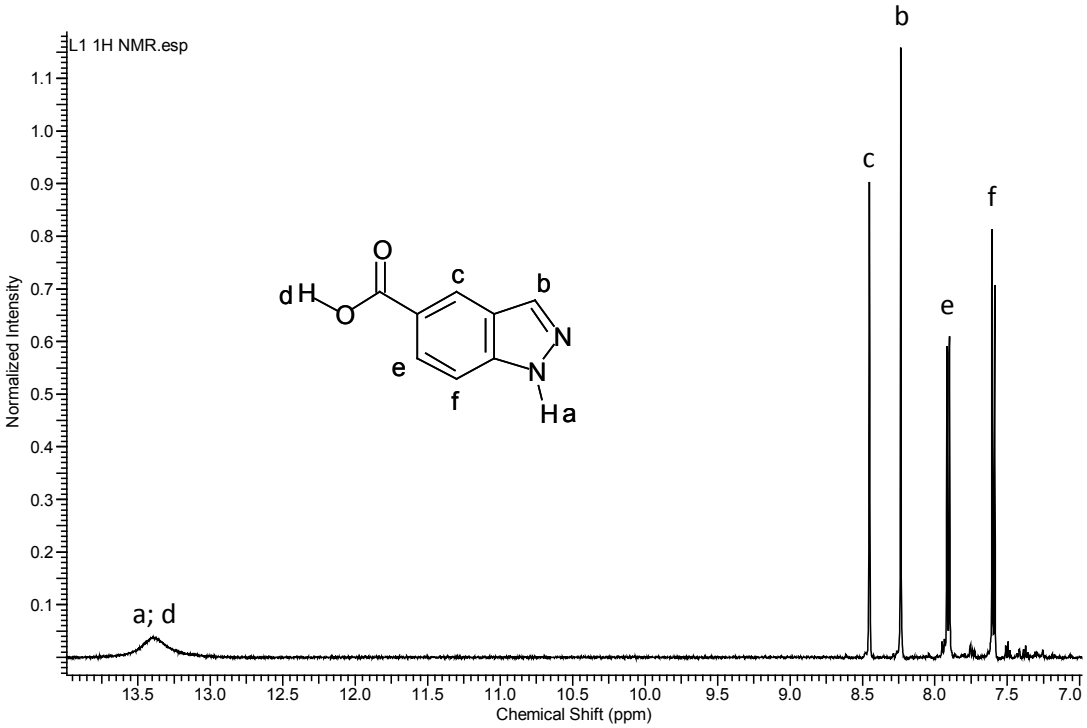

Figure S2: ^{13}C NMR spectrum of $\mathbf{H_2L}$ (d_6-DMSO @ 125 MHz):

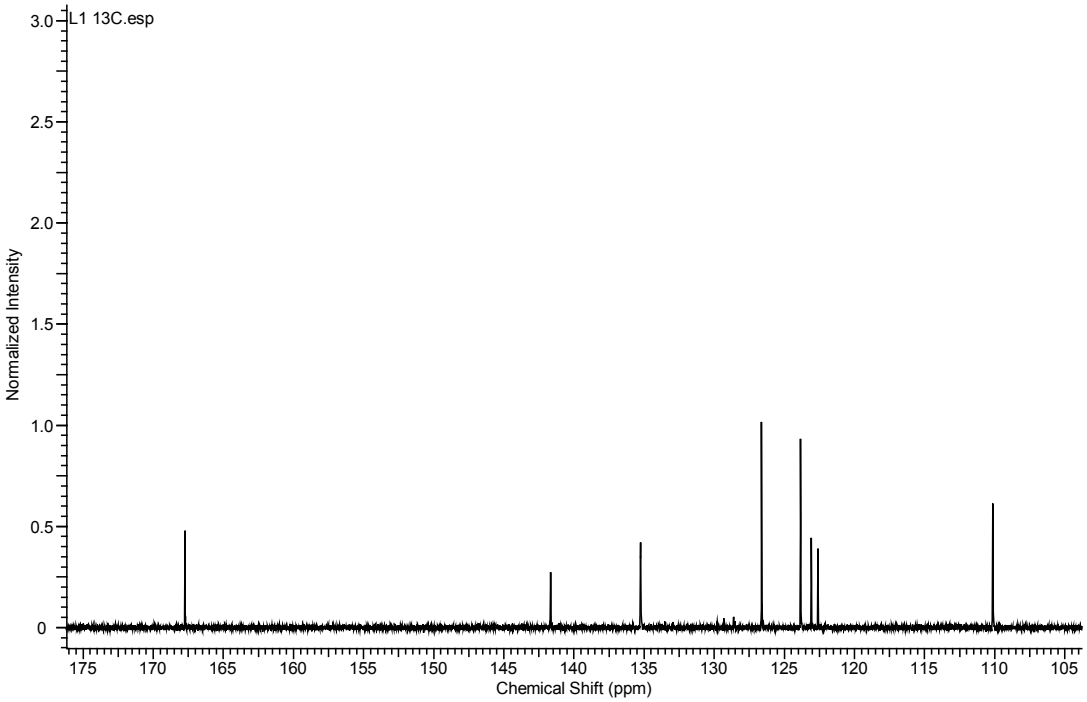

This journal is © The Royal Society of Chemistry 2012

X-ray Crystallography

Refinement data are presented in Table S1. X-ray crystallographic data collection and refinement was carried out with an Oxford ATLAS area detector using Cu/Kα radiation from an Oxford SuperNova dual microsource instrument (λ = 1.5418 Å). All structures were solved using direct methods with SHELXS [4] and refined on F^2 using all data by full matrix least-squares procedures with SHELXL-97 [5] within OLEX-2 [6]. Non-hydrogen atoms were refined with anisotropic displacement parameters. Hydrogen atoms were included in calculated positions with isotropic displacement parameters 1.2 times the isotropic equivalent of their carrier atoms. The functions minimized were $\Sigma w(F^2_o - F^2_c)$, with $w=[\sigma^2(F^2_o)+aP_2+bP]^{-1}$, where $P=[\max(F_o)^2+2F^2_c]/3$.

Structure solution revealed the presence of channels within **1**. The electron density present in these channels was so diffuse as to prevent explicit modelling of the solvent guests, and the use of the SQUEEZE routine within PLATON [7] was not required due to the high degree of accuracy evident in the unmodified data. However, SQUEEZE was used to estimate the void contents on electron density grounds and suggested 427 electrons per unit cell, equivalent to approximately 47 electrons per copper, consistent with the equivalent of 2.5 methanol molecules, 4.5 water molecules, or a combination of the two, and accounting for *ca.* 36% of the unit cell volume. The structure of **1** after heating (designated **1A**), returned near identical crystallographic data to **1** (Table S1). However the void contents calculated by SQUEEZE were reduced to 37 electrons per unit cell and with markedly improved refinement statistics, suggesting significant desolvation of the channels whilst maintaining the open network structure.

This journal is © The Royal Society of Chemistry 2012

Table S1 Crystallographic data for **1** and **1A**

Compound reference	**1**	**1A**
Chemical formula	$C_{16}H_{10}CuN_4O_4$	$C_{16}H_{10}CuN_4O_4$
Formula Mass	385.82	385.82
Crystal System	Trigonal	Trigonal
a/Å	33.6525(6)	33.6966(8)
b/Å	33.6525(6)	33.6966(8)
c/Å	4.80132(11)	4.78817(13)
α/°	90.00	90.00
β/°	90.00	90.00
γ/°	120.00	120.00
Unit cell volume/Å^3	4708.98(16)	4708.4(2)
Temperature/K	120.0(1)	120.0(1)
Space group	$R\bar{3}$	$R\bar{3}$
No. of formula units per unit cell, *Z*	9	9
No. of reflections measured	26227	9622
No. of independent reflections	1883	2092
R_{int}	0.0274	0.0221
Final R_1 values ($I > 2\sigma(I)$)	0.0379	0.0265
Final $wR(F^2)$ values ($I > 2\sigma(I)$)	0.1331	0.0697
Final R_1 values (all data)	0.0396	0.0284
Final $wR(F^2)$ values (all data)	0.1348	0.0711
μ /mm^{-1}	1.686	1.686

Table S2: Hydrogen bond parameters for **1**.

D–H···A	**d(D–H)/Å**	**d(H–A)/Å**	**d(D–A)/Å**	**D–H···A/°**
N3–H3···O13^{i}	0.860(18)	1.99(3)	2.721(2)	143(3)

Symmetry operator: i) +X, +Y, 1+Z

Table S3: Hydrogen bond parameters for **1A**.

D–H···A	**d(D–H)/Å**	**d(H–A)/Å**	**d(D–A)/Å**	**D–H···A/°**
N3–H3···O13^{i}	0.847(15)	1.970(17)	2.7219(15)	147.3(18)

Symmetry operator: i) 1-X, 1-Y, 1-Z

This journal is © The Royal Society of Chemistry 2012

Figure S3: Schematic view of the two interpenetrated networks in **1** viewed approximately down the crystallographic *c*-axis, choosing Cu(II) centres as nodes.

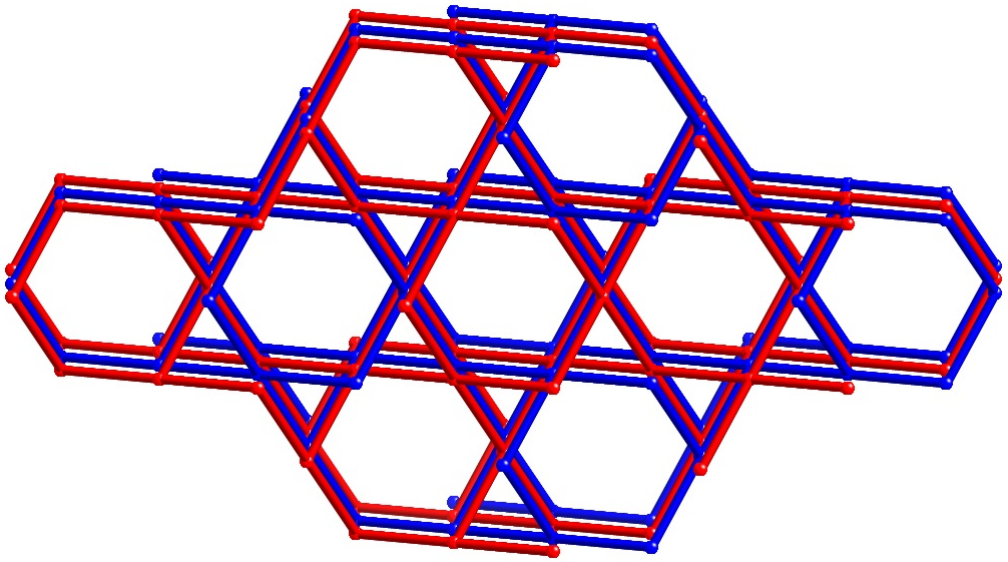

This journal is © The Royal Society of Chemistry 2012

Figure S4: Thermogravimetric analysis trace for **1** showing weight % (green) and δW/δT (blue).

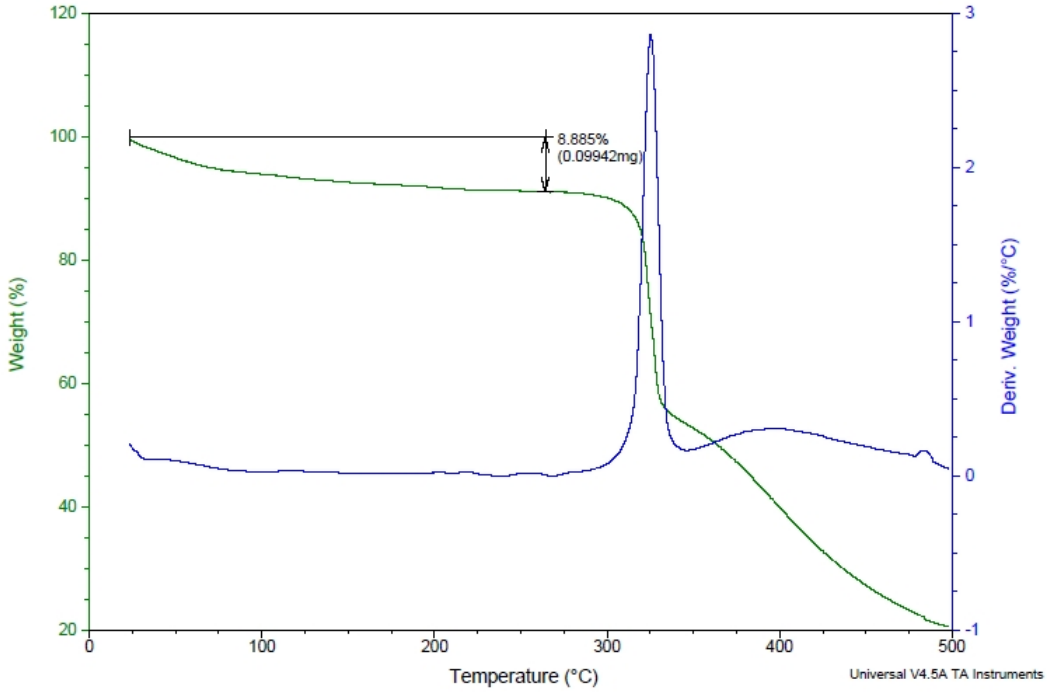

This journal is © The Royal Society of Chemistry 2012

Figure S5: X-ray Powder Diffraction Pattern for freshly prepared **1** (red), dehydrated sample **1A** (green) and pattern simulated from single crystal data (blue).

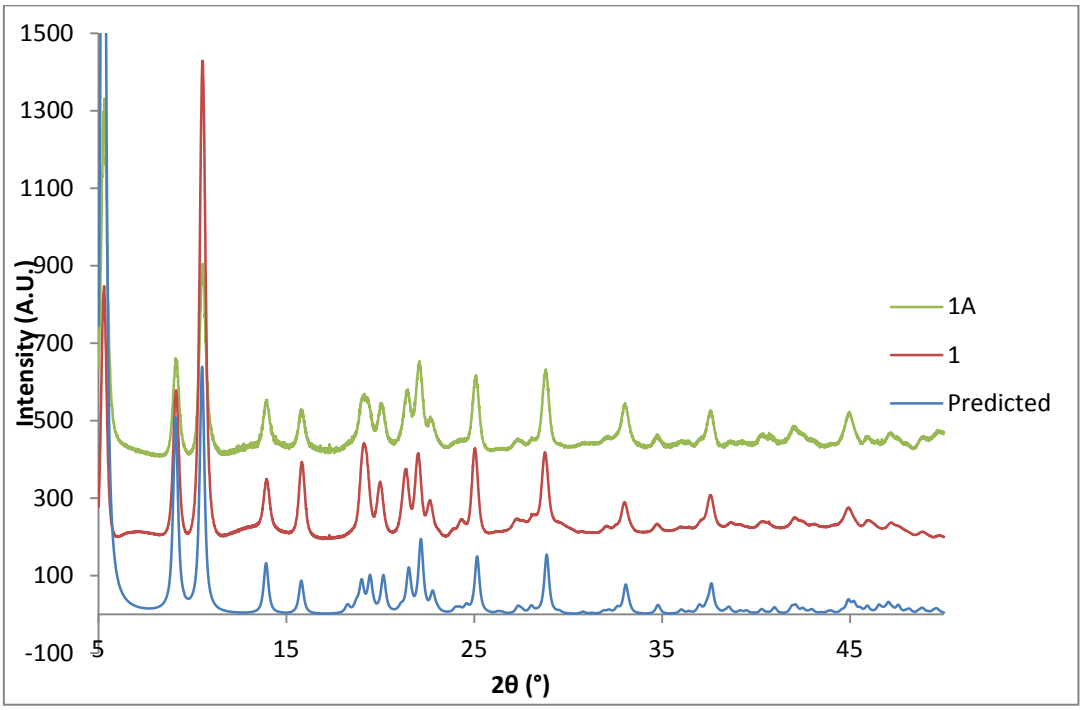

This journal is © The Royal Society of Chemistry 2012

Gas sorption experimental and isosteric heat of sorption calculations

A sample of **1** was baked at 150 °C under dynamic vacuum overnight. The dried sample on which the gas sorption studies were undertaken had a mass of 103.6 mg. Between isotherm measurements the sample was re-baked at 150 °C for 2 hours.

Gas sorption data were measured using a Sieverts-type BELsorp-HP automatic gas sorption apparatus (BEL Japan Inc.). Ultra-high purity CH_4, CO_2, and He were used for the sorption studies.

Corrections were made for non-ideal gas behaviour at high pressures of each gas at each measurement and reference temperature. Source data were obtained from the NIST fluid properties website. [8]

Sample compartment temperatures between 258 K and 298 K were controlled by a Julabo F25-ME chiller/heater. A calibrated external Pt100 temperature probe monitored the flask temperature. Samples were kept at the measurement temperature for a minimum of 1 hr after the desired temperature had been achieved to allow thermal equilibrium to be attained before data measurement commenced.

Isosteric heats of sorption were calculated using least-squares fitting of a virial-type thermal adsorption equation that modelled lnP as a function of amount of surface excess of gas sorbed over all measurement temperatures. [9]

This journal is © The Royal Society of Chemistry 2012

Figure S6. Sorption enthalpy versus CO_2 sorbed by **1** calculated using the Virial method on the data obtained from the 258 and 273 K isotherms.

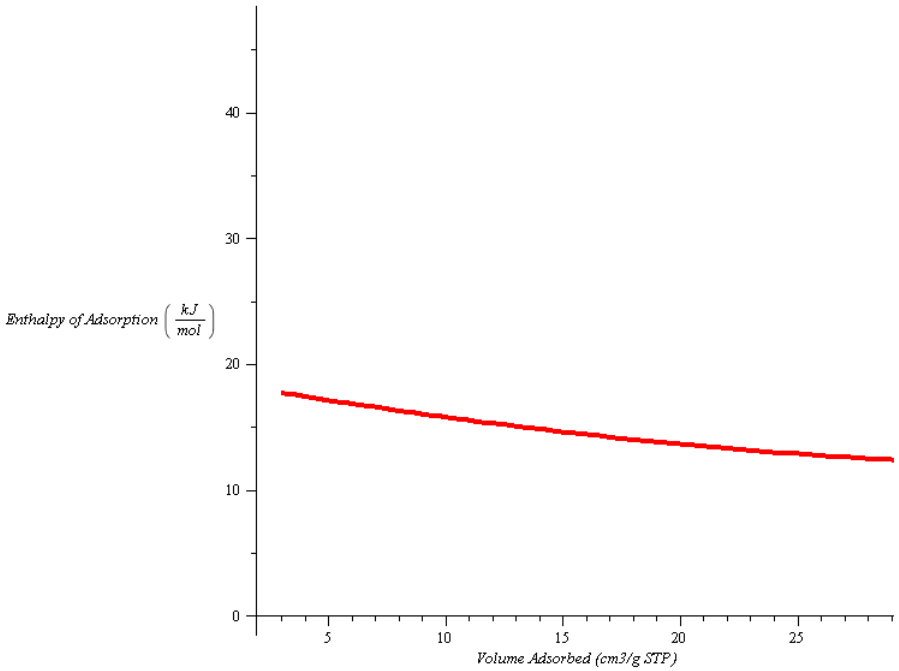

This journal is © The Royal Society of Chemistry 2012

Figure S7. 273K isotherms for CO_2 (yellow diamonds) and methane (black circles) sorption by **1**.

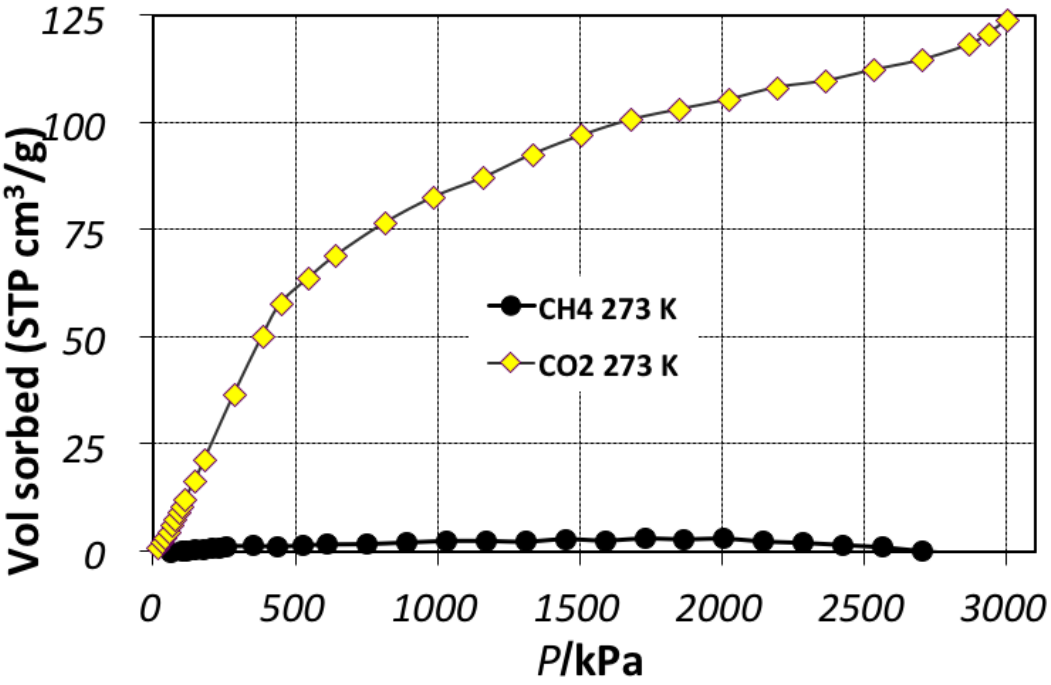

Figure S8. H_2 Isotherms collected at 258K (blue circles), and 273K (red squares)

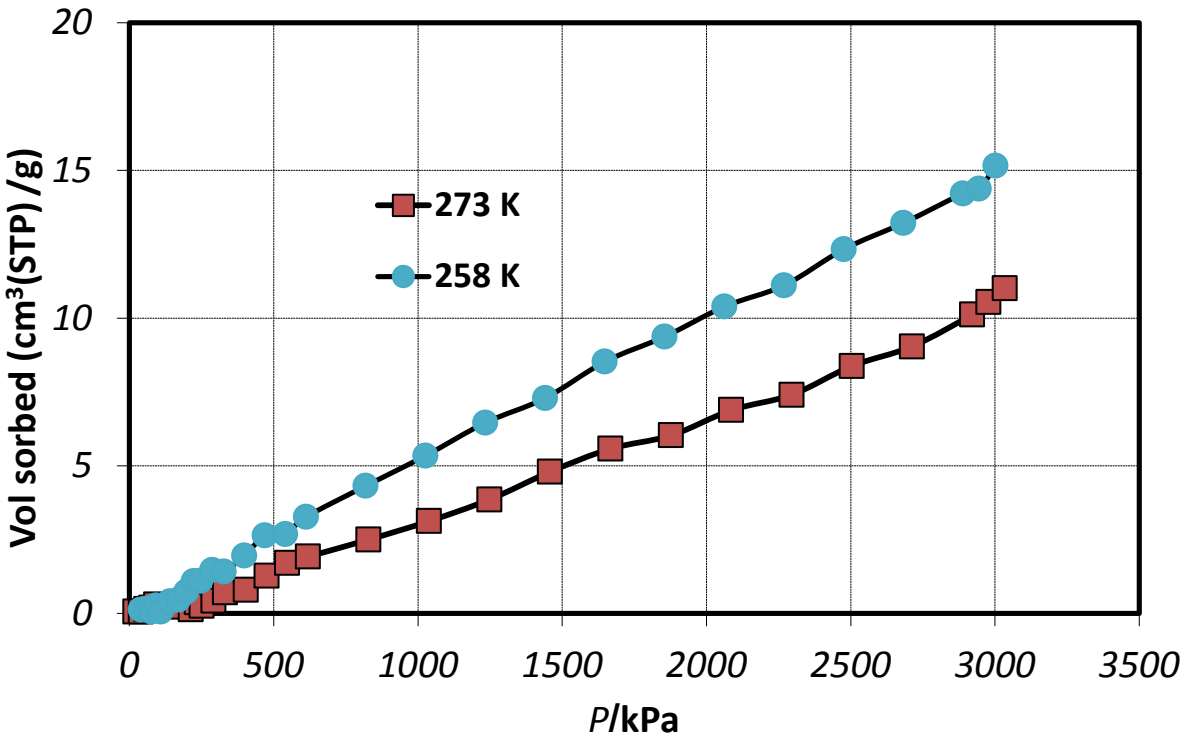

Figure S9. N_2 isotherm collected at 77K

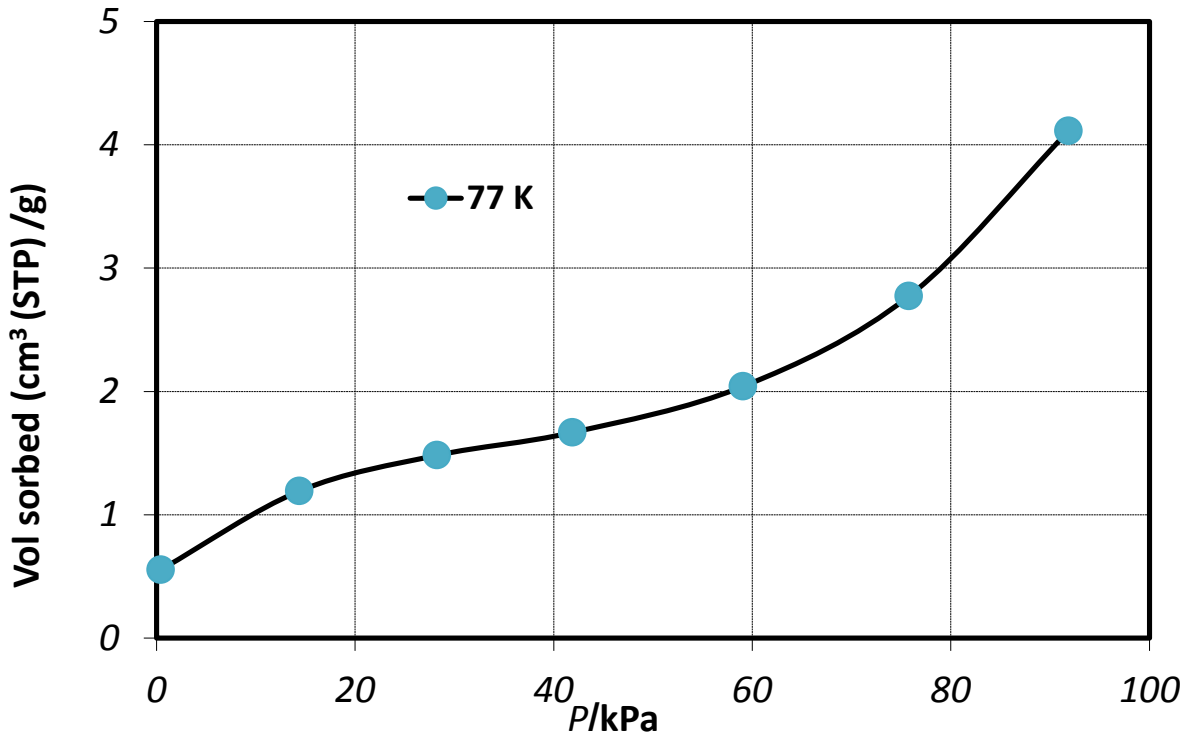

Figure S10. High-resolution CO_2 isotherm @ 273 K.

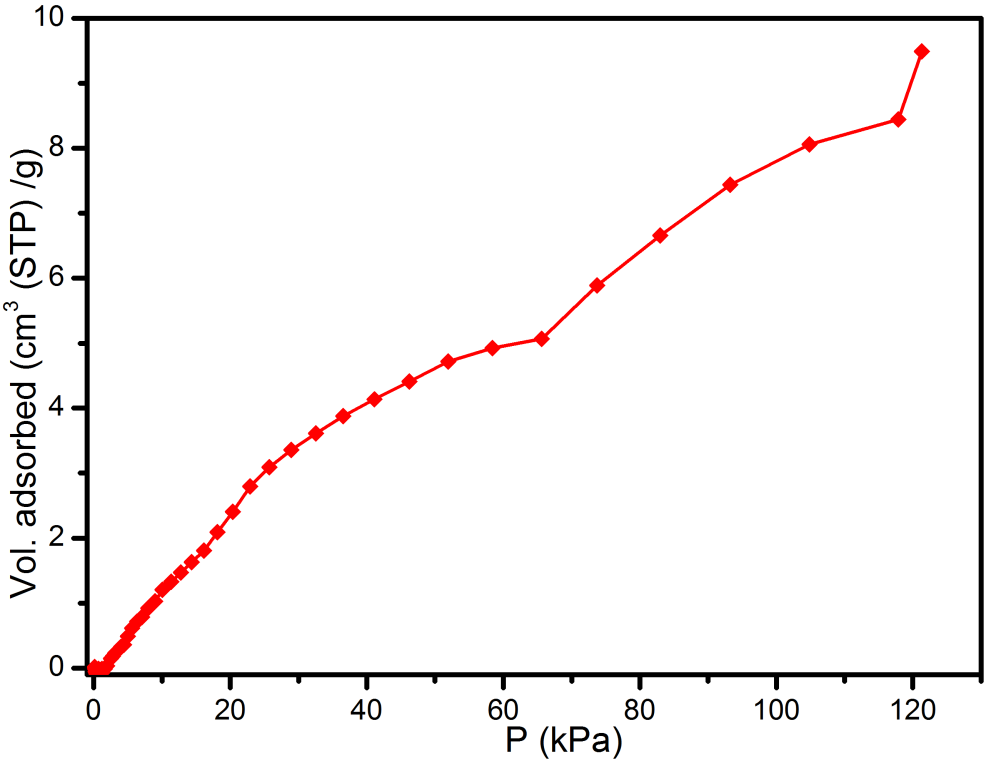

This journal is © The Royal Society of Chemistry 2012

Simulation Methods and Models

The adsorption of pure CO_2 was simulated by grand canonical Monte Carlo (GCMC) method. Because the chemical potentials of adsorbate in adsorbed and bulk phases are identical at thermodynamic equilibrium, GCMC simulation allows one to relate the chemical potentials of adsorbate in both phases and has been widely used for the simulation of adsorption. The framework atoms are kept frozen during simulation. The LJ interactions were evaluated with a spherical cutoff equal to half of the simulation box with long-range corrections added; the Coulombic interactions were calculated using the Ewald sum method. The number of trial moves in a typical GCMC simulation was 2×10^7, though additional trial moves were used at high loadings. The first 10^7 moves were used for equilibration and the subsequent 10^7 moves for ensemble averages. Five types of trial moves were attempted in GCMC simulation, namely, displacement, rotation, and partial regrowth at a neighboring position, entire regrowth at a new position, and swap with reservoir. Unless otherwise mentioned, the uncertainties are smaller than the symbol sizes in the figures presented.

Experimental adsorption isotherm is usually reported in the excess amount N_{ex} while simulation gives the absolute amount N_{ab}. To convert from N_{ab} to N_{ex}, we use

$$N_{ex} = N_{ab} - \rho_b V_{free} \qquad (1)$$

where ρ_b is the density of bulk adsorbate calculated using Peng-Robinson equation of state, V_{free} is the free volume in adsorbent available for adsorption and is estimated from

$$V_{free} = \int_V \exp\left[-u_{ad}^{He}(r)/k_B T\right] dr \qquad (2)$$

where u_{ad}^{He} is the interaction between Helium and adsorbent, in which σ_{He} = 2.58 Å and ε_{He}/k_B=10.22 K.[10] Note that the free volume detected by helium is temperature dependent, and usually the room temperature is chosen. The ratio of free volume V_{free} to the occupied volume V_{total} gives the porosity ϕ of adsorbent.

Canonical ensemble (NVT) simulation is performed to estimate the isosteric heat of adsorption at infinite dilution. A single adsorbate molecule is subjected to three types of trial moves employed in the NVT simulation, namely, translation, rotation and regrowth. The isosteric heat at infinite dilution is calculated from

$$q_{st}^0 = RT - \left(U_{total}^0 - U_{intra}^0\right) \qquad (3)$$

where U_{total}^0 is the total adsorption energy of a single molecule with adsorbent and U_{intra}^0 is the intramolecular interaction of a single gas molecule in bulk phase.

The adsorbate CO_2 was mimicked as three-site model to account for the quadrupole moment. The C–O bond length in CO_2 was 1.18 Å and the bond angle ∠OCO was 180°. The charges on C and

O atoms were +0.576e and –0.288e (e = 1.6022 $\times 10^{-19}$ C the elementary charge), resulting in a quadrupole moment of -1.29×10^{-39} C·m^2. The LJ parameters for CO_2 were σ_C = 2.789 Å, ε_C = 29.66 K, σ_O = 3.011 Å, ε_O = 82.96 K.[11]

The experimentally determined crystal structure was used in simulations. Atomic partial charges are calculated based on fragmental cluster using density functional theory (DFT) as implemented in DMol^3.[12] The DFT calculation was performed on a cluster model cleaved from the unit cell. The PW91 functional along with the Double-ξ numerical polarization (DNP) basis set was used in the DFT calculations, which is comparable to 6-31G(d,p) Gaussian-type basis set. DNP basis set incorporates p-type polarization into hydrogen atoms and d-type polarization into heavier atoms. From the DFT calculations, the atomic charges were evaluated by fitting to the electrostatic potential using the Merz-Kollman (MK) scheme as listed in Table S4.[13,14] The interactions of gas-adsorbent and gas-gas were modeled as a combination of pairwise site-site Lennard-Jones (LJ) and Coulombic potentials. The LJ potential parameters of the framework atoms are adopted from and Dreiding force field.[15] However, the DREIDING force field parameter is not available for Cu atom, thus the parameter from the Universal force field (UFF)[16] was adopted. To account for inflection in CO_2 isotherm the DREIDING force field parameters were rescaled to match the experimental isotherm. This type of adjustment of force field parameters has been widely done in previous works.[17-19] Table S5 lists the set of LJ parameters used in this study. The Lorentz-Berthelot combining rules were used to calculate the cross LJ interaction parameters.

Table S4. Atom charges in **1** and the atom types are labelled in Figure S11.

Atom Type	Cu1	N2	N3	O12	O13	C4
Charge	0.918	-0.238	-0.226	-0.690	-0.604	0.236
Atom Type	C5	C6	C7	C8	C9	C10
Charge	-0.363	-0.040	-0.056	-0.322	0.116	-0.116
Atom type	C11	H3	H5	H6	H8	H10
Charge	0.684	0.346	0.219	0.174	0.219	0.202

Figure S11. Atomic types in **1**.

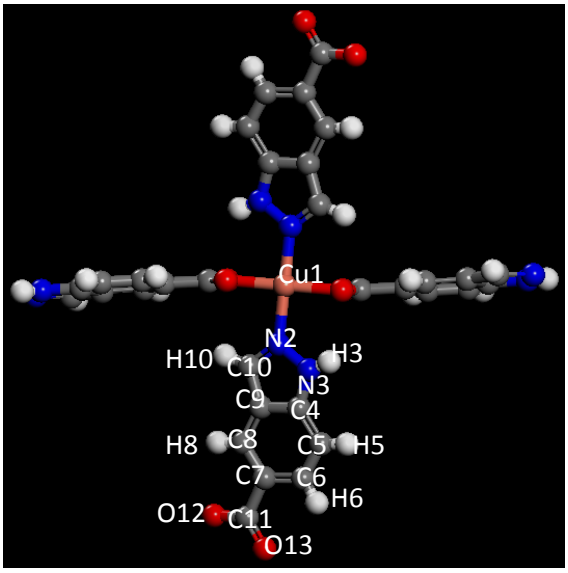

Table S5. LJ potential parameter for the framework atoms in **1**.

Atom type	Cu	C	O	N	H
σ (Å)	3.11	3.30	2.88	3.10	2.71
ε / k_B (K)	2.52	39.9	40.2	29.2	6.38

This journal is © The Royal Society of Chemistry 2012

Results and Discussions

Figure S12 shows the adsorption isotherm for CO_2 at 298 K in **1**. The simulated results agree fairly well with the experimental data over the entire pressure.

Figure S12. Adsorption isotherm of CO_2 in **1** at 298 K in (a) log scale (b) linear scale

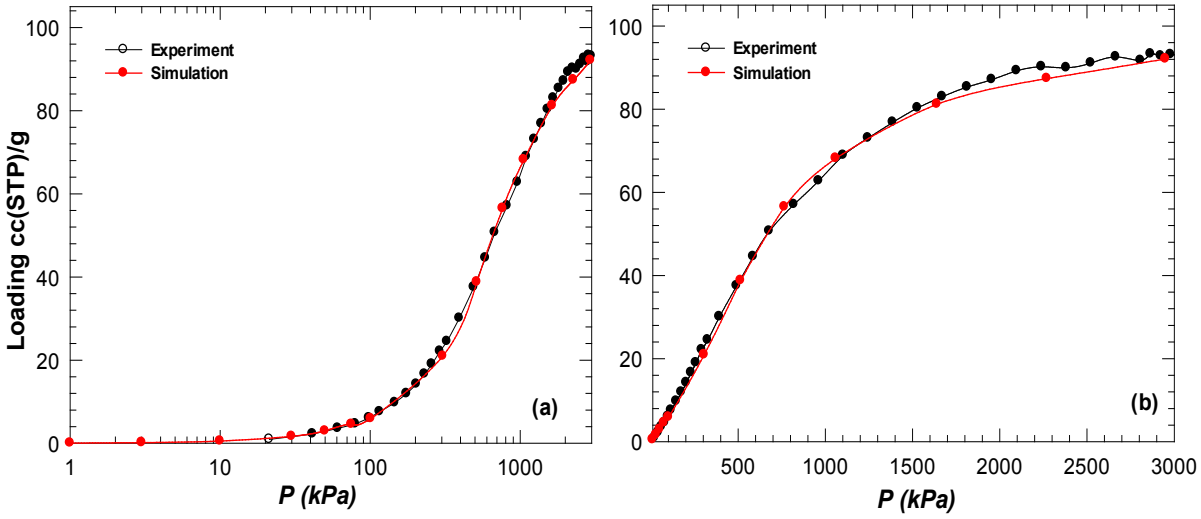

To better understand the location of adsorption sites, Figure S13 shows the radial distribution functions $g(r)$ between CO_2 and the framework atoms in **1**.

$$g_{ij}(r) = \frac{\Delta N_{ij} V}{4\pi r^2 \Delta r N_i N_j}$$

where r is the distance between species i and j, ΔN_{ij} is the number of species j around i within a shell from r to $r + \Delta r$, V is the volume, N_i and N_j are the number of species i and j. A pronounced peak in $g(r)$ is observed at r = 4.2 Å between CO_2 and framework atoms C5 and C6. This confirms that CO_2 interacts with the phenyl ring more strongly than the other framework atoms. The isosteric heat of adsorption predicted from simulation is around -15 kJ/mol at zero loading which is slightly lower than the experimentally observed value of -17.5 kJ/mol.

Figure S13. Radial distribution functions between CO_2 and framework atoms (a) C5 and C6 (b) Cu1, N2, N3, O12 and O13.

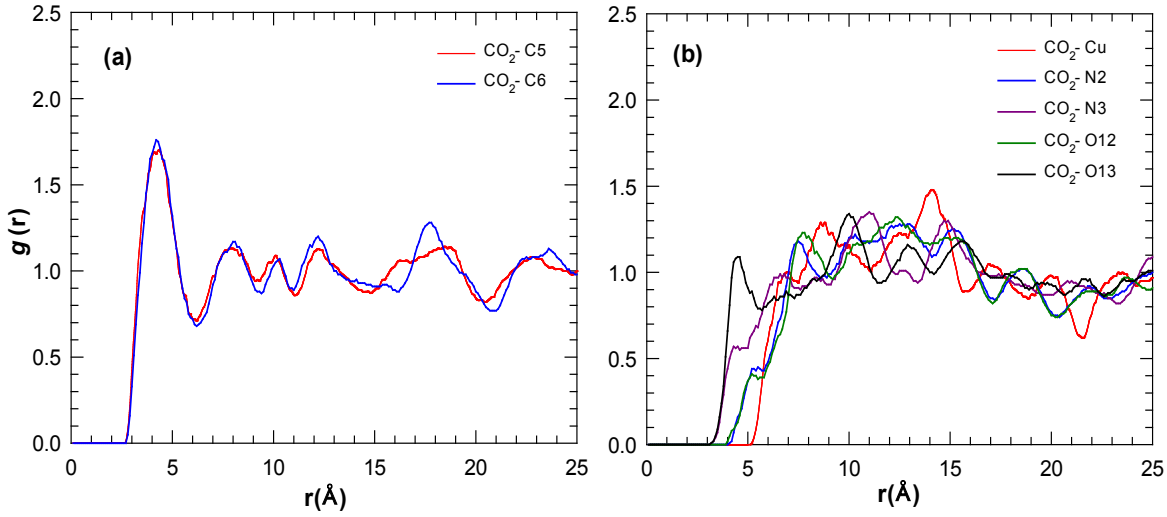

Figure S14 shows the density contours of CO_2 at 10 kPa in **1**. The contours are viewed from the (100) plane and generated by accumulating 200 equilibrium configurations. CO_2 molecules are primarily adsorbed in the pore centres.

Figure S14. Density contours of CO_2 adsorption at 10 kPa in **1**.

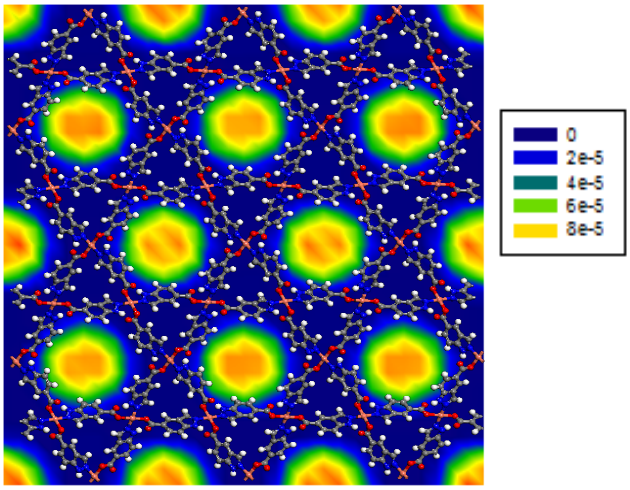

This journal is © The Royal Society of Chemistry 2012

References

[1] S. Ram and R. E. Ehrenkaufer, *Tetrahedron Lett.,* 1984, **25**, 3415-3418

[2] G. Bartoli, M. Bosco, R. D. Pozzo and M. Petrini, *Tetrahedron,* 1987, **43**, 4221-4226.

[3] C. Rüchardt and V. Hassmann, *Liebigs Ann. Chem.,* 1980, 908-927.

[4] G.M. Sheldrick, *Acta Crystallogr., Sect. A.,* 2008, **64**, 112.

[5] G.M. Sheldrick, SHELXL-97, Programs for X-ray Crystal Structure Refinement, University of Gottingen, 1997.

[6] O.V. Dolomanov, L.J. Bourhis, R.J. Gildea, J.A.K. Howard and H. Puschmann, OLEX2: A complete structure solution, refinement and analysis program *J. Appl. Cryst.,* 2009, **42**, 339-341.

[7] A. L. Spek, *Acta Crystallogr. Sect. D- Biol. Crystallogr.* 2009, **65**, 148-155.

[8] http://webbook.nist.gov/chemistry/fluid/

[9] L. Czepirski, J. Jagiello, *Chem. Eng. Sci*. 1989, **44**, 797–801

[10] Hirschfelder, J. O.; Curtiss, C. F.; Bird, R. B. *Molecular Theory of Gases and liquids*; John Wiley: New York, 1964.

[11] Hirotani, A.; Mizukami, K.; Miura, R.; Takaba, H.; Miya, T.; Fahmi, A.; Stirling, A.; Kubo, M.; Miyamoto, A. *Appl. Surf. Sci.* **1997**, *120*, 81-84.

[12] *Materials Studio, 6.0 ed.;* Accelrys, San Diego, 2011.

[13] Singh, U. C.; Kollman, P. A. *J. Comput. Chem.* **1984**, *5*, 129-145.

[14] Besler, B. H.; Merz, K. M.; Kollman, P. A. *J. Comput. Chem.* **1990**, *11*, 431-439.

[15] Mayo, S. L.; Olafson, B. D.; Goddard, W. A. *J. Phys. Chem.* **1990**, *94*, 8897-8909.

[16] Rappe, A. K.; Casewit, C. J.; Colwell, K. S.; Goddard, W. A.; Skiff, W. M. *J. Am. Chem. Soc.* **1992**, *114*, 10024-10035.

[17] Dubbeldam, D.; Calero, S.; Vlugt, T. J. H.; Krishna, R.; Maesen, T. L. M.; Beerdsen, E.; Smit, B. *Phys. Rev. Lett.* **2004**, *93*.

[18] Thornton, A. W.; Dubbeldam, D.; Liu, M. S.; Ladewig, B. P.; Hill, A. J.; Hill, M. R. *Energy Environ. Sci.* **2012**, *5*, 7637-7646.

[19] Zhang, W.; Huang, H.; Zhong, C.; Liu, D. *PhysChemChemPhys* **2012**, *14*, 2317-2325.